JET PRODUCTION IN e^+e^- ANNIHILATION AND DECAYS OF THE Y(9.46) RESONANCE - RESULTS FROM PLUTO -

Gerhard Knies
Deutsches Elektronen-Synchrotron DESY
Notkestr. 85, D-2000 Hamburg 52

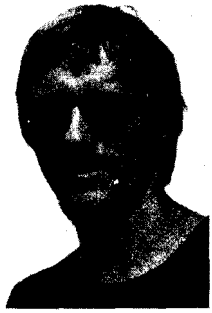

Abstract

Electron positron annihilation events, measured by the PLUTO detector at energies Q from 3.6 to 17 GeV at DORIS and PETRA are used to study the properties of hadronic jets. We find good agreement with the picture of $q\bar{q}$ pair production and subsequent fixed $p_\perp$ fragmentation. Evidence for b quark production is discussed. The Y(9.46) decays are investigated in the context of the 3-gluon decay expected from QCD, on the basis of charged tracks. We observe an increase of track multiplicity and of sphericity as expected for a 3-gluon decay. A new measure for flatness as the consequence of an original planar configuration is defined. The Y events are compared to events from the nearby continuum, and from model calculations for $q\bar{q}$ jets, for phase space and for a 3-gluon decay, assuming gluon fragmentation like quark fragmentation. The 3-gluon decay model compares well with the data in many respects.

I. Introduction

Electron-positron annihilation experiments in recent years have been very instrumental in extending our knowledge on the fundamental fermions, both the quarks and the leptons. The annihilation into hadrons in particular is important for our understanding of the interactions between quarks and provides a fruitful testing ground for quantum chromodynamics. The most important results are the observation of new quark flavours through the formation of resonances (J/ψ, Υ) and thresholds in the total cross section, the proportionality of the total cross section to the square of the electric charges of the quarks above threshold at the respective energies, and the production of jets as a result of the limited $p_\perp$ hadronization of quark pairs[1].

In this talk we will review the experiments carried out with the PLUTO detector on e^+e^- annihilation into hadrons at the storage rings DORIS and PETRA, and discuss the significance of the results. In section II we deal with the production of jets at energies from 3.6 to 17 GeV, and in section III the evidence for a 3-gluon decay of the Υ is reviewed.

Fig. 1 shows the layout of the storage rings DORIS and PETRA and the synchrotron DESY at the DESY site in Hamburg. The storage rings have been described elsewhere[2]. DORIS has been running at energies from 1.5 to 5 GeV per beam, and PETRA can at present be operated at energies from ~ 5 GeV up to ~ 14 GeV per beam.

The PLUTO detector is operated by the PLUTO collaboration[3]. The detector is shown in fig. 2, and is described elsewhere[4]. It has a superconducting magnet with a solenoidal field of 1.7 tesla and 14 cylindrical proportional chambers for tracking, and proportional tube chambers outside the return yoke for μ-identification. The PLUTO detector has been taking data at DORIS since 1976. In 1977 shower counters were added. In 1978 it was moved to PETRA and a forward spectrometer as well as more hadron absorber iron and a second layer of μ-chambers were added. Table 1 gives a break down of the data collected at DORIS and PETRA.

In fig. 3 we show the total cross section for the annihilation of e^+e^- into hadrons, together with an account of the expected contribution from the various quark flavours.

Table 1 Data collected by PLUTO

Data taking storage ring	E_{cm} GeV	L • T nb^{-1}	No. of events	$E_{neutral}$
1976	3.1 (J/ψ)	50	28 000	
	3.6	600	3 500	with lead converters
DORIS	3.7 (ψ')	160	30 000	
	4.03	750	7 500	
	4.4	440	3 500	
	5.0	700	4 200	
1978	7.7	250	1 000	
	9.4	180	470	with shower counters
	9.46 (Y)	190	1 870	
1979	13	42.6	96	
PETRA	17	88.3	108	

II. Production of jets in e^+e^- annihilation

II.1. How visible are jets?

In fig. 4a two multiprong events at CMS energies of 26 GeV are shown as examples of obvious collinear jets. In fig. 4b a jetlike event is sketched together with the definitions of variables used for the quantitative description of jets. The collinear jet character of events becomes visible when the average of the longitudinal momenta along the jet axis becomes larger than the average of the transverse momenta. In perfectly isotropic events with a very large multiplicity we find for any axis $\langle p_\parallel \rangle = \langle p_\perp \rangle / \sqrt{2}$. When multiplicity is limited, e. g. $\langle n_{charged} \rangle \lesssim 10$ there is in general an axis with respect to which $\langle p_\parallel \rangle > 1/(\sqrt{2}) \cdot \langle p_\perp \rangle$, even though there is no genuine jet formation. For example at Q = 9.46 GeV, charged tracks from phase-space events yield $\langle p_\parallel \rangle \sim 1.2 \cdot \langle p_\perp \rangle$. Experimentally jets become a clearly visible and dominant feature only at energies of 9.4 GeV, where for the observed average values we read from fig. 5

$$\langle p_\parallel \rangle = 2 \langle p_\perp \rangle .$$

Below 5 GeV, the jet character of events is traceable only on a statistical basis by comparing experimental distributions like the sphericity or the inclusive particle momenta to phase space and jet models. From these facts the energy scale of jet formation can be roughly deduced: It takes an energy of more than ~ 4 GeV for each quark jet to become a clearly visible pattern in 2 jet events, whereas 2 GeV per jet are clearly not enough to make the jet pattern identifiable.

II.2. Quantitative topological properties of jets

The physics questions of interest in the context of jet production in e^+e^- annihilation are:

(1) Do $q\bar{q}$ pairs fragment into hadrons with a constant, limited $p_\perp$ when the jet energies grow?

(2) Are there any effects caused by passing the threshold for new quark flavours - in the energy range under discussion here for the b-quark?

(3) Are there QCD effects like the expected gluon bremsstrahlung?

Both (2) and (3) lead to less jetlike events, with larger $\langle p_\perp \rangle$ or sphericity. Fig. 6 shows the diagrams describing these processes.

In (2) the weak decays of the pair of heavy quarks bring in an additional transverse momentum, and the Lorentz boost is smaller than for the lighter quarks.

In (3) the gluon bremsstrahlung introduces an additional $p_\perp$ to the quark and gluon before hadronization. Therefore, in one of the two hemispheres we can expect a broadening of the jet, or even the formation of 2 jets[5]. A separation of new heavy flavour production and gluon bremsstrahlung can then be based on the following features:

(i) jet broadening is symmetric (heavy flavour) or asymmetric (gluon),

(ii) heavy flavour production adds new large $p_\perp$ (sphericity) events whereas gluon bremsstrahlung increases large $p_\perp$ and reduces small $p_\perp$ events,

(iii) the number of leptons grows in new heavy flavour events,

(iv) the energy dependence of these effects shows a sudden threshold for new heavy flavours and a gradual growth for gluon bremsstrahlung[5].

II.3. Jet measures and corrections

For describing the properties of jets we are going to use the following quantities based on $p_\perp$ and $p_\parallel$:

sphericity	S	$= \text{Min}\ \frac{3}{2} \sum_i p_\perp^2 / \sum_i p^2$
thrust	T	$= \text{Max} \sum_i \lvert p_\parallel \rvert / \sum_i \lvert p \rvert$
jet opening angle	$\sin^2\delta$	$= \sum E_i \cdot \sin^2\delta_i / \sum E_i$

The summing index i in our analysis runs over all charged tracks of an event[6]. Energies are calculated using pion masses. In theoretical calculations, the origi-

nal quark axis is the direction of reference for $p_\perp$ and $p_\parallel$. In real events, the direction of reference are the sphericity and thrust axes as reconstructed from the charged tracks. The angles between sphericity and thrust axes are plotted in fig. 7. The experimental quantities $p_\perp$ and $p_\parallel$ are distorted by using the experimental sphericity or thrust axis rather than the 'true' quark axis, by using charged tracks only, by track measurement errors, by detector acceptance, by trigger acceptance and off-line event selection, and by photon bremsstrahlung in the initial state.

The impact of all these effects on the topological quantities mentioned above has been investigated with simulated jet events. The observed values of the topological quantities can then be corrected. The corrections for $\langle p_\perp \rangle$ are typically of the order of -10 %. The jet events were generated[7] along the lines of the fixed $p_\perp$ ($\langle p_\perp \rangle$ = 0.3 GeV/c to the primary hadrons) non perturbative quark fragmentation model of Feynman and Field[8] (FF model). This model explicitly includes u, d and s quarks only, but it describes the experimental $p_\perp$ distribution also above charm threshold. The results we are going to show are corrected, if not labelled "observed".

II.4. Results

The properties of the transverse momenta are shown in figs. 8a ($p_\perp^2$ distribution) and 8b (average $p_\perp$). We observe that $\langle p_\perp \rangle$ indeed grows a little bit, by ~ 20 MeV/c when going from 7.7 to 9.4 GeV, and from 9.4 to 13 and 17 GeV. The latter change can be understood from crossing over the b threshold. We find the same $\langle p_\perp \rangle$ at 13 and 17 GeV within 20 MeV/c. In fig. 9 $\langle p_\perp \rangle$ for different intervals of $x_\parallel$ is shown at 7.7 and 17 GeV together with the expectation from the FF model. At 17 GeV the data seem to have larger $\langle p_\perp \rangle$ at more or less all $x_\parallel$, than expected without $b\bar{b}$ production.

The distribution of longitudinal momentum in fig. 10 shows significant deviations from the FF parameterization for $x_\parallel > 0.4$. These deviations however are independent of energy: the FF parameterization always predicts larger fluxes beyond $x_\parallel = 0.4$ than are observed. The lengthening of the plateau in rapidity when going from 7.7 to 17 GeV (fig. 11a) goes along with the expectation from the FF model, and its average value has the expected dependence on the energy, namely $\langle y \rangle \propto \ln Q$ (fig. 11b).

Now we turn to variables that combine $p_\perp$ and $p_\parallel$. In fig. 12a we show the energy dependence of the average values for the opening angle of energy flow in a jet, $\langle \sin^2\delta \rangle$, and in fig. 12b and c we show $\langle S \rangle$ and $\langle 1-T \rangle$ together with the expectation

from the non perturbative FF model and another non perturbative model that includes $c\bar{c}$ and $b\bar{b}$ thresholds[9]. It is obvious that including a $b\bar{b}$ threshold (at Q = 10 GeV) is favoured by the data. But there is no significant disagreement without it. This can be seen in fig. 13 where we compare the experimental sphericity distribution to the expectation[9] from u, d, s and c quark production at 9.4 GeV and to the expectations[9] with and without b quark production at 13 and 17 GeV. With the present statistics, there is no clear evidence that the b quark contribution is needed to describe the data.

Finally, in fig. 14 we show the polar angle distribution of (thrust-) jet axis at 7.7 and 9.4 GeV. It agrees with the expected $1+\cos^2\vartheta$ behaviour.

In summary we find

(1) $\langle p_\perp \rangle$, $\langle S \rangle$, $\langle 1-T \rangle$ show an energy dependence when going from Q = 7.7 to Q = 17 GeV that is consistent with the production and non perturbative fragmentation of $q\bar{q}$ pairs with a fixed $\langle p_\perp \rangle$ = 0.3 GeV/c to the primary hadrons.

(2) the agreement is improved when the production and weak decay of $b\bar{b}$ quark pairs is included.

(3) the $x_\parallel$ distribution is consistent with scaling, the rapidity plateau increases and $\langle y \rangle$ grows proportional to ln Q.

(4) We find no need or evidence for jet broadening from gluon bremsstrahlung.

The apparent absence of QCD effects agrees with a recent analysis of the size of jet broadening due to gluon radiation[10]. In fig. 15 we show the predicted dependence of $\langle p_\perp \rangle$ on Q. The result is that QCD effects are still marginal at Q $\lesssim$ 15 GeV, and that only at Q $\sim$ 30 GeV do they become prominent.

III. Decay properties of the Y(9.46)

III.1. Introduction

According to QCD the strong decay of the Y(9.46) vector meson is an annihilation of the $b\bar{b}$ bound state into gluons. Annihilation into 1 gluon is forbidden by the colour of gluons, and annihilation into a colour white 2 gluon state by charge conjugation. Annihilation into 3 and more gluons however is possible. Assuming the 3 gluon annihilation (fig. 16) to be the dominant strong decay[11] one may then expect, depending on details of gluon hadronization, to observe 3-jet events.

There is, however, the competing electromagnetic (E.M.) decay (fig. 16): $Y \to \gamma \to$ hadrons. The branching fraction for this decay mode can be obtained from

the E.M. decay $Y \to \gamma \to \mu^+\mu^-$ via the relation $B(Y \to \gamma \to \text{hadrons}) = R \cdot B(Y \to \gamma \to \mu^+\mu^-)$, with $R = 4$ and $B(Y \to \mu^+\mu^-) = (2.2 \pm 2.0)$ %.

$$B(Y \to \gamma \to \text{hadrons}) \approx 10\ \%,$$

$$B(Y \xrightarrow{\text{direct}} \text{hadrons}) = (1 - B(Y \to \gamma \to \text{hadrons}) \approx 90\ \%.$$

Hence we find experimentally that ~ 90 % of the Y decay into hadrons is not through 1 γ, and the question we want to study here is whether there is some evidence for a 3-gluon decay mode.

III.2. The Y data

In fig. 17 we show the total cross section for $e^+e^- \to$ hadrons at energies around the Y mass. The width of the Y peak is due to the energy spread of the storage ring DORIS. In the Y peak range, i. e. "on" the Y, we have 3 different contributions to multihadron final states, as indicated in the diagrams of fig. 18. These are the 1 γ annihilation events from the continuum (diagram a), the E.M. decay of the Y (diagram b), both with the same properties as those "off" the Y, and the events from the "direct" decay of the Y (diagram c). If interference effects can be neglected the "direct" cross section reads

$$\sigma_{dir} = \sigma_{on} - \sigma_{off}\left(\frac{\sigma^{\mu\mu}_{on} - \sigma^{\mu\mu}_{off}}{\sigma^{\mu\mu}_{off}} + 1\right). \qquad \text{(III.1)}$$

In the following analysis we discuss the properties of the events from the direct Y decays[12]. The corresponding "direct" distributions (in any variable x) can be obtained by subtracting out the "1 γ" content from the "on" Y data bin by bin, using the measurements "off" Y. Including the luminosities "on" and "off" Y eq. (III.1) leads to

$$\left.\frac{dN}{dx}\right|_{dir} = \left.\frac{dN}{dx}\right|_{on} - 1.32 \left.\frac{dN}{dx}\right|_{off}. \qquad \text{(III.2)}$$

III.3. How to look for 3 g structure of Y decays

We can distinguish several levels of evidence for a 3-gluon decay mode of the Y.

(1) The clearest evidence is seeing events with 3 separated jets by eye.

(2) The 3 jets are not fully separated, but quantitative 3-jet measures reveal an underlying 3-jet pattern in a statistical way.

(3) The 3 jets are not fully separated, but the events still have a flat shape as remains of the original planar configuration of the 3 gluons.

(4) The original planar 3-jet configuration is washed out completely during fragmentation, e. g. the two lower energetic jets never separate, but the jettiness of the events is degraded and track multiplicity is increased as compared to the 2-jet events off Y. On the other hand the events are still different from uncorrelated final states.

In the following sections we discuss these levels of evidence in the sequence (1), (4), (3) and (2). In doing so we compare the Y events to observed and to simulated 2-jet events off the Y, to simulated spherical events assuming a direct decay of the Y into pions and kaons (phase space), and to events simulating a 3-gluon decay[13] of the Y. Here we assume that gluons fragment like quarks, and a matrix element[14] describing the Dalitz plot density for the decay of the Y into 3 massless gluons.

III.4. Are there 3-jet events visible by eye?

Seeing jets requires already more than 3 GeV energy per jet for collinear quark jets as we have seen in section II. Gluon jets may well be broader - how broad is a very interesting question for gluon fragmentation - and a 3-jet pattern is more complicated. Therefore, we expect that clearly more than 3 GeV are needed per jet before we see a 3-jet structure "by eye". For 3 gluon Y decays, however, QCD predicts[14] for the lowest energy jet an average energy of 2 GeV. In fact, the events do not exhibit a visible 3-jet pattern.

III.5. Are the Y events different from continuum jets and from phase space?

In fig. 19 we show the (observed) sphericity and thrust average values for the Y events and for "continuum" events at several energies. Table 2 gives the values for simulated phase space and 3-gluon events at the Y energy. It is clear that the Y events are less jet like than the 9.4 GeV events, and at the same time more "jetty" than phase space events. Sphericity and thrust average values of the Y agree with the 3-gluon simulation, and so do the sphericity and thrust distribution (fig. 20). This indicates that quark and gluon fragmentation may be similar. However, here we also notice limits to the agreement between this specific 3-gluon model and the Y data: The 3-gluon average values for $p_\perp$ and $p_\parallel$ (table 2) are both significantly larger than in the Y data. In comparison to the continuum jet events we find that $\langle p_\parallel \rangle$ of Y events is sizably smaller, whereas $\langle p_\perp \rangle$ is not different. The charged multiplicity increases from 6.3 ±0.4 (continuum) to 8.0 ±0.3 at the Y.

III.6. Are Y events flat?

In the preceeding paragraph we have seen that Y events are more similar to 2-jet events than isotropic decays. Here we will discuss if the data provide more specific evidence for a 3-jet origin of the Y events. Even if the 2 less energetic

Table 2: Mean observed values for thrust, sphericity, Q_1, F , $|p_{out}|$, $p_\perp$, $p_{\shortparallel}$, acoplanarity, triplicity, and θ_1. For definitions see text. The data on Υ(9.46) and on continuum (9.40) are compared to events simulating $q\bar{q}$ jets, 3-gluon decay and phase space. Also the corrected average charge multiplicity for the data is included.

	2 jet (9.40) MC	2 jet (9.40) data	Υ(9.46) data	Υ(9.46) MC	phase space MC
1-<T>	0.16	0.18 ± .01	0.24 ± .01	0.24 ± .01	0.27 ± .01
<S>	0.22	0.27 ± .01	0.39 ± .01	0.35 ± .03	0.46 ± .02
$<Q_1>$	0.030	0.036± .002	0.056± .003	0.050± .005	0.067± .005
<F>	0.69 ±.01	0.72 ± .01	0.70 ± .01	0.68 ± .01	0.68 ± .01
$<\|p_{out}\|>$(MeV/c)	0.115	0.118± .003	0.129± .003	0.140± .006	0.177± .006
$<p_\perp>$ (MeV/c)*	0.32	0.33 ± .01	0.34 ± .01	0.38 ± .01	0.47 ± .01
$<p_{\shortparallel}>$ (MeV/c)*	0.72	0.62 ± .02	0.49 ± .01	0.55 ± .01	0.58 ± .01
<A>	0.084	0.099± .005	0.15 ± .01	0.14 ± .01	0.16 ± .01
1-<T3>	0.059	0.063± .002	0.085± .003	0.089± .001	0.098± .001
$<\theta_1>$ (^{o})	73.7	76.4 ±1.2	85.0 ±1.2	87.6 ± .5	91.7 ± .3
$<N_{CH}>$		6.3 ± .4	8.0 ± .3		

*) with respect to thrust axis.

jets from a 3-jet final state are not separated track by track in space, but still have an effective partial separation on the average, then these events are no longer rotationally symmetric around their sphericity axis. They would not be round, but flat. Flatness by itself may not prove a 3-jet pattern, but it is a necessicity. Now we introduce a quantitative definition of flatness. A convenient frame work is provided by the eigenvalues λ_i of the momentum tensor[12]. The quantities

$$Q_k = 1 - \frac{2\lambda_k}{\lambda_1 + \lambda_2 + \lambda_3} = \frac{\sum_i (p^i_{k\shortparallel})^2}{\sum_i (p^i)^2} \qquad \text{(III.3)}$$

measure the fraction of the squares of the momentum components of all tracks along the direction k. They are bound to $Q_1 + Q_2 + Q_3 = 1$, and with $\lambda_1 \geq \lambda_2 \geq \lambda_3$ we have $Q_3 \geq Q_2 \geq Q_1$. They are related to sphericity by

$$Q_1 + Q_2 = \frac{2}{3} S. \qquad \text{(III.4)}$$

The sum of Q_1 and Q_2 measures the jettiness of an event, with $Q_1 + Q_2 = 0$ for extreme jets, and $Q_1 + Q_2 = \frac{2}{3}$ for perfect spherical events.

The flatness of an event can be characterized by Q_1 and Q_2. If $Q_1 = Q_2$ then we find along all directions perpendicular to the sphericity axis the same value for the sum of squares of momentum components. We then have an event with a circular cross section perpendicular to the sphericity axis. Events with $Q_1 < Q_2$ have an elliptical cross section. All events with the same ratio Q_1/Q_2 have the same elliptical shape. We therefore define as flatness

$$F = 1 - Q_1/Q_2 \qquad \text{(III.5)}$$

with F = 1 for extreme flat events ($Q_1 = 0$) and F = 0 for no flatness (cylindrical symmetry, $Q_1 = Q_2$). Quantities based on momentum components along a single direction only, like $|p_{out}|$, acoplanarity[15], or Q_1, do not directly measure the flatness of an event.

Events with a finite number of final state particles in general will have a flatness F > 0. In our analysis we want to find out, whether the Y events exhibit a flatness that exceeds the bias from small track statistics.

In table 2 we compare the average values of F for the Y events, the 3-gluon MC, the phase space MC, the 9.4 GeV events and the F.F. MC. We find a consistent value of $\langle F \rangle$ in all 5 cases. In two of the models (phase space and FF) there is no inherent flatness. Flatness there is nothing but a bias from fluctuations due to low track multiplicities. The fact that the 3 gluon simulated events also yield the same average value for flatness tells us that at Y energies the bias toward flatness from low track statistics is much stronger than any genuine effect from a 3-gluon decay, if gluons fragment similar to quark jets.

So we find the result that in the process of fragmentation no significant flatness is retained in the charged tracks as a remnant of an original planar configuration In analogy to section III.5, where sphericity ($\sim Q_1 + Q_2$) in the continuum events was found significantly smaller than in the Y events, but $\langle p_\perp \rangle$ values of both cases were consistent, we find here that Q_1 is significantly smaller for the continuum events, but $\langle p_{out} \rangle$, where p_{out} is the momentum component along the Q_1 axis, is consistent in both types of events. The prediction from the 3-gluon model for the average value and for the distribution of p_{out} (fig. 21) agrees very nicely with the Y data - in contrast to $\langle p_\perp \rangle$ where agreement is marginal.

III.7. Direct test for a 3-jet pattern

A method[16] designed to find a possible 3-jet pattern directly uses the quantity triplicity:

$$T_3 = \max\{|\sum_{i\,c_1} \vec{p}_i| + |\sum_{i\,c_2} \vec{p}_i| + |\sum_{i\,c_3} \vec{p}_i|\} / \sum_{all} |\vec{p}_i| \qquad \text{(III.6)}$$

It can be looked at as thrust in 3 directions (see fig. 22). The subsets c_ℓ of tracks have no tracks in common, are not empty, and contain all tracks of the event. Since we here are using charged tracks only, we introduce an additional momentum conserving vector such that

$$\sum_i \vec{p}_i(\text{charged}) + \vec{p}(\text{balance}) = 0. \qquad \text{(III.7)}$$

Including $\vec{p}$(bal.) makes sure that the 3-direction vectors g_ℓ (see fig. 22) fall into a plane and that for the angles θ_i we have $\sum \theta_i = 360^o$. T_3 ranges between $T_3 = 1$ for perfect 3-jet and perfect 2-jet events, and $T_3 = 3 \cdot \sqrt{3}/8 = 0.65$ for perfect spherical events. The quantity thrust allows then to distinguish between perfect 2-jet ($T = 1$) and perfect 3-jet ($T < 1$) events. The directions of the momentum sums of those subsets c^*_ℓ yielding the maximum in (III.6) are taken as the jet directions.

Of course, in 3-jet events with overlapping jets the method yields biased jet directions. This effect is accounted for by using simulated events from the 3-gluon model.

The results we are going to show here represent an unpublished intermediate step of the analysis as of the date of this talk. A more complete analysis including neutral particles has been performed in the meantime[17].

In fig. 22 we show the distribution of T_3 and θ_1, the opening angle between the 2 jets with the lower thrust, of the Y and 9.4 GeV events in comparison to the 3 respective models. For both variables we find good agreement between the Y-data and the 3g-MC events, and a clear difference to the phase space as well as to the continuum data. As a check we also show the results for $q\bar{q}$-MC which agree very well with those from the continuum events.

Since $\theta_1 + \theta_2 + \theta_3 = 360^o$, and also $\theta_1 \leq \theta_2 \leq \theta_3$, the 2-dimensional triangle plot in fig. 23 shows the correlated $\theta_1 - \theta_2 - \theta_3$ distribution. Again we find that Y decays and simulated 3-jet events populate the θ plane in a very similar way, and are different from simulated phase-space events. Other models without a 3-jet structure, e. g. more complicated phase-space models including resonances are not ruled out.

III.8. Summary

We have prepared a sample of Y decays where contributions from the electromagnetic decays into $q\bar{q}$ events are subtracted, and performed a first analysis using charged tracks only.

We have compared the Y decays to events from the nearby continuum, and to simulated events from the FF quark-antiquark pair fragmentation model, from a phase-space model and from a model for a 3-gluon QCD decay, with gluon fragmentation like quark fragmentation.

There are clear differences between the Y data and the continuum events:

(i) larger charged particle multiplicity;

(ii) reduced jettiness (as measured by thrust and sphericity).

These effects are qualitatively expected as a difference between 3 gluon and $q\bar{q}$ decays.

The Y data are also incompatibel with a simple phase-space model.

A comparison between the 3-gluon model predictions and the Y data shows good agreement in many details, like sphericity, thrust, triplicity, the angles between the 3-jet directions (as obtained by the triplicity method) and a new quantity proposed to measure flatness, as a consequence of an original planar configuration. This latter quantity, however, shows no differences for the average flatness of Y events, phase-spase events, continuum events and $q\bar{q}$ simulated events.

I appreciate the help and the discussions I had with many colleagues at DESY when preparing this report.

References

1) See for example:
G. Hanson, Proceedings of the XIIIth Rencontres de Moriond, ed. Trân Thanh Vân (1978) and references therein.

2) PETRA proposal, DESY, Hamburg 1976.

3) PLUTO Collaboration:
Ch. Berger, H. Genzel, R. Grigull, W. Lackas, F. Raupach, W. Wagner, A. Klovning, E. Lillestöl, E. Lillethun, J.A. Skard, H. Ackermann,

G. Alexander, F. Barreiro, J. Bürger, L. Criegee, H.C. Dehne, R. Devenish, G. Flügge, G. Franke, W. Gabriel, Ch. Gerke, G. Horlitz, G. Knies, E. Lehmann, H.D. Mertiens, B. Neumann, K.H. Pape, H.D. Reich, B. Stella, U. Timm, P. Waloschek, G.G. Winter, S. Wolff, W. Zimmermann, O. Achterberg, V. Blobel, L. Boesten, H. Kapitza, B. Koppitz, W. Lührsen, R. Maschuw, R. van Staa, H. Spitzer, C.Y. Chang, R.G. Glasser, R.G. Kellog, K.H. Lau, B. Sechi-Zorn, A. Skuja, G. Welch, G.T. Zorn, A. Bäcker, S. Brandt, K. Derikum, C. Grupen, H.J. Meyer, M. Rost, G. Zech, T. Azemoon, H.J. Daum, H. Meyer, O. Meyer, M. Rössler, D. Schmidt, K. Wacker

4) L. Criegee et al., Proc. 1973 Int. Conf. on Instrum. for HEP, Frascati 1973; PLUTO Collaboration, J. Burmester et al., Phys. Lett. 64B (1976) 369.

5) There is a flood of literature on this topic. A very recent analysis with references to other work can be found in: P. Hoyer, P. Osland, H.G. Sander, T.F. Walsh, and P.M. Zerwas, DESY-79/21 (April 1979).

6) An analysis including the neutral energy is forthcoming, for data taken at energies of $Q \geq 7.7$ GeV.

7) We adapted a computer program written by H.G. Sander (unpublished).

8) R.D. Field, R.P. Feynman, Nucl. Phys. B136 (1978) 1.

9) A. Ali, J.G. Körner, J. Willrodt, G. Kramer, DESY-79/16 (February 1979).

10) See the paper quoted in ref. 5.

11) T. Appelquist, H.D. Politzer, Phys. Rev. Lett. 34 (1979) 43 and Phys. Rev. D12 (1975) 1404.

12) Most of the following results are already published by the PLUTO collaboration: Ch. Berger et al., Phys. Lett. 82B (1979) 449.

13) K. Koller, T.F. Walsh, Phys. Lett. B72 (1977) 227, B73 (1978) 504 and Nucl. Phys. B140 (1978) 449; T.A. de Grand et al., Phys. Rev. D16 (1977) 3251; S. Brodsky et al., Phys. Lett. B73 (1978) 203; H. Fritzsch, K.H. Streng, Phys. Lett. B74 (1978) 90; K. Hagiwara, Nucl. Phys. B137 (1978) 164; R. Gatto, I. Vendramin, Univ. of Geneva Preprint UGVA/DPT/10-182 (1978); S.Y. Pi et al., Phys. Rev. Lett. 41 (1978) 142.

14) K. Koller, H. Krasemann, T.F. Walsh, DESY-78/37 (1978), Z. f. Phys. C, in print.

15) A. de Rujula, J. Ellis, E.G. Floratos, M.K. Gaillard, Nucl. Phys. B138 (1978) 387.

16) S. Brandt, H.D. Dahmen, Z. Physik C1 (1979) 61.

17) PLUTO Collaboration, Ch. Berger et al., DESY 79/43 (1979) and Proceedings of the International Conference on High Energy Physics (A. Zichichi, ed.), Geneva 1979.

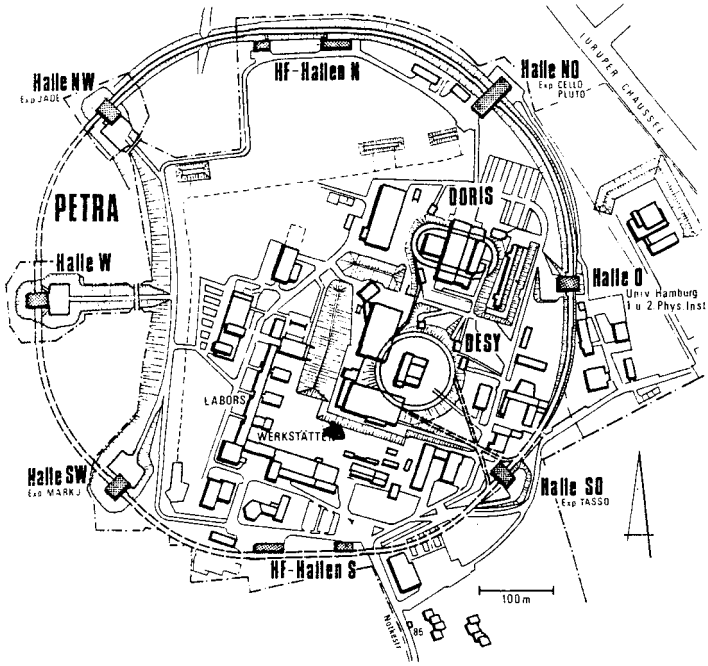

Fig. 1: DESY site at Hamburg

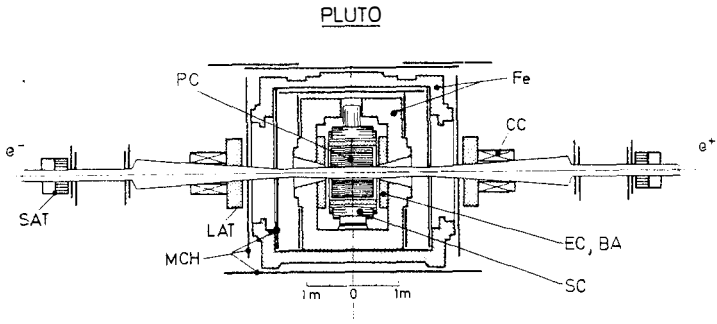

Fig. 2: PLUTO detector. Cross section along the e^+e^- beam axis. SAT = small angle tagger (20 - 70 mrad, luminosity monitor), LAT = large angle tagger (70 - 250 mrad), EC and BA = endcap and barrel shower counters (>250 mrad). MCH = chambers for muon identification. Fe = 60 + 40 cm iron for hadron absorption. SC = superconducting coil (1.6 tesla, solenoidal field), PC = 14 cylindrical proportional chambers for tracking.

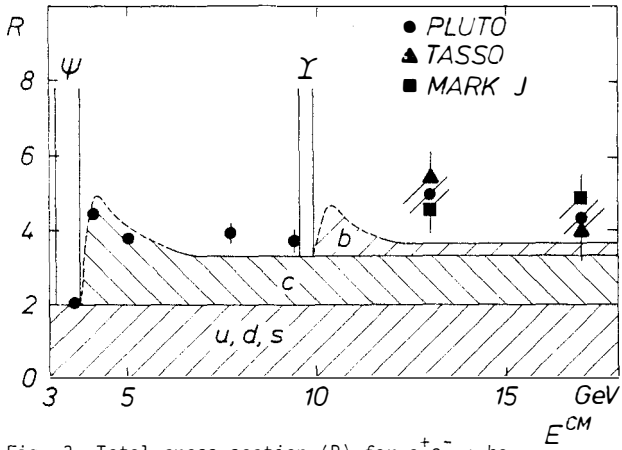

Fig. 3: Total cross section (R) for $e^+e^- \to$ hadrons as measured by PLUTO. At 13 and 17 GeV also measurements by TASSO and MARK J are included. The shaded regions represent the contributions from the indicated quark flavors.

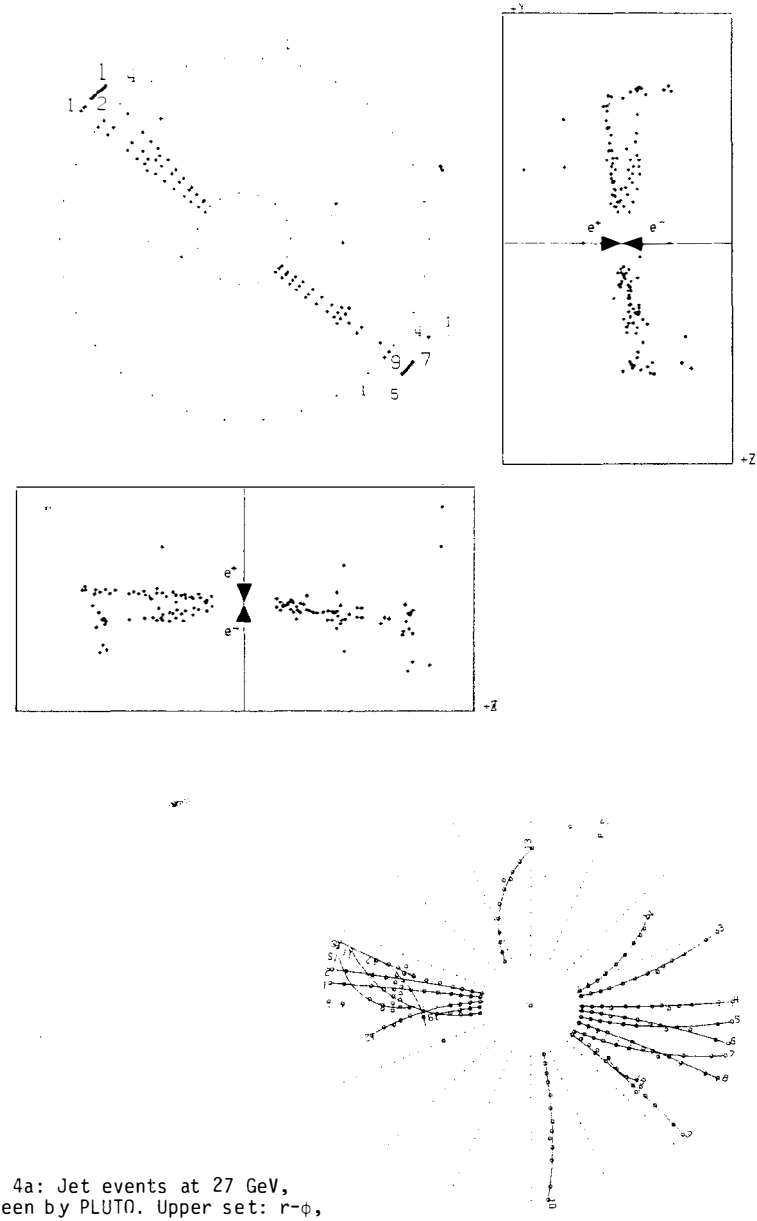

Fig. 4a: Jet events at 27 GeV, as seen by PLUTO. Upper set: r-ϕ, y-z and x-z projections. Lower picture, r-ϕ projection with fitted tracks.

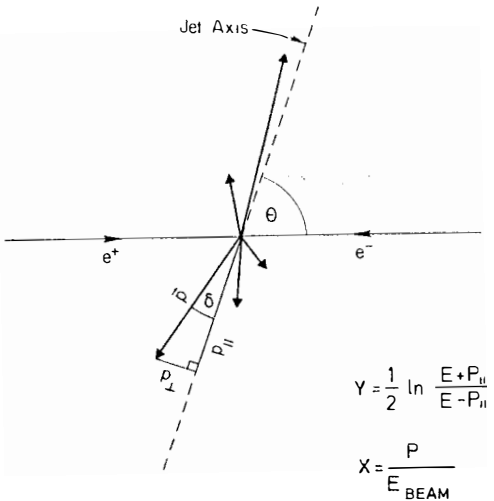

Fig. 4b: Definition of jet variables.

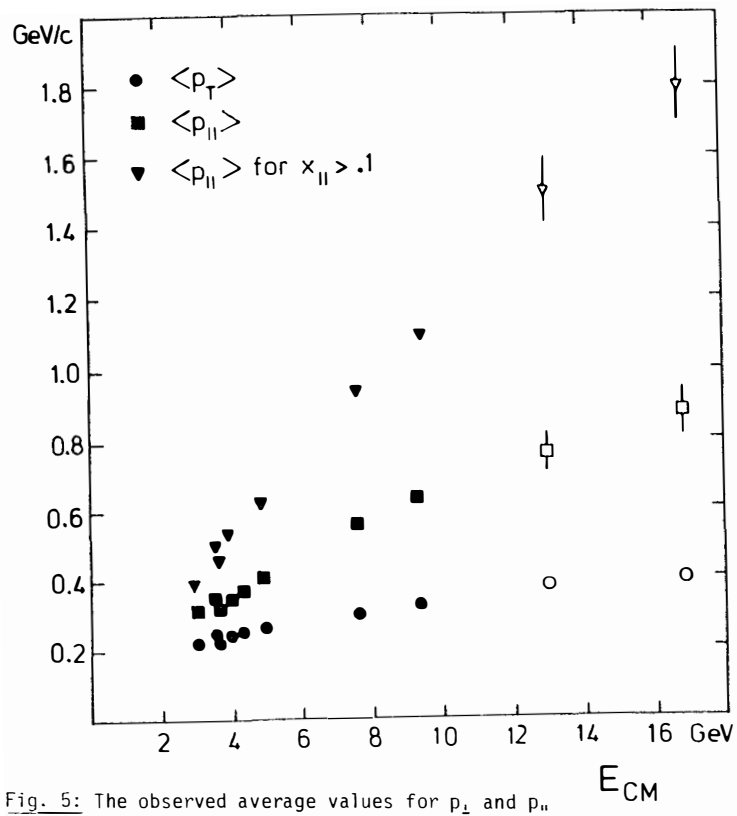

Fig. 5: The observed average values for $p_\perp$ and $p_\parallel$

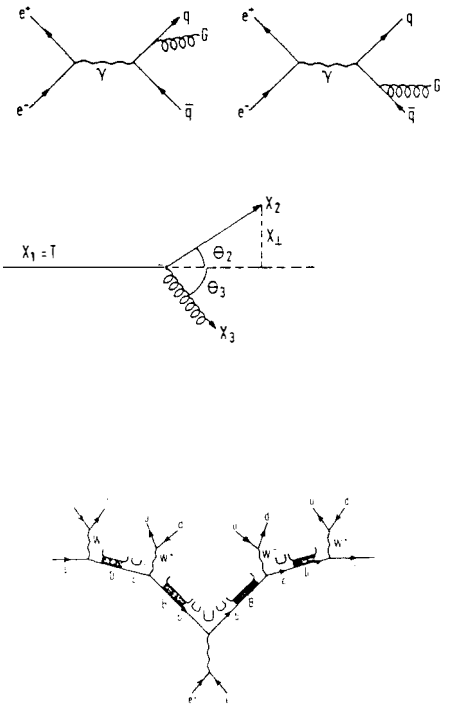

Fig. 6: Diagrams for first order QCD process (gluon radiation) and a decay chain in $b\bar{b}$ production.

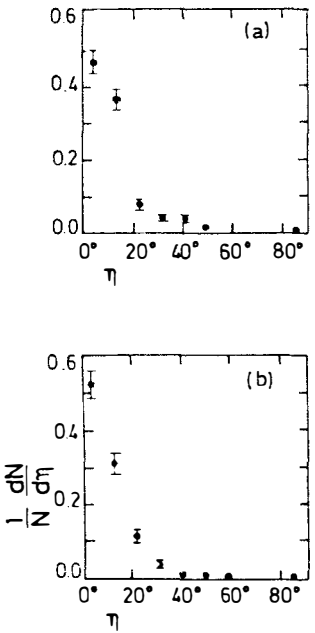

Fig. 7: (a) Angle η between reconstructed thrust and sphericity axes. (b) Angle η between largest momentum and sphericity axis at Q = 9.4 GeV.

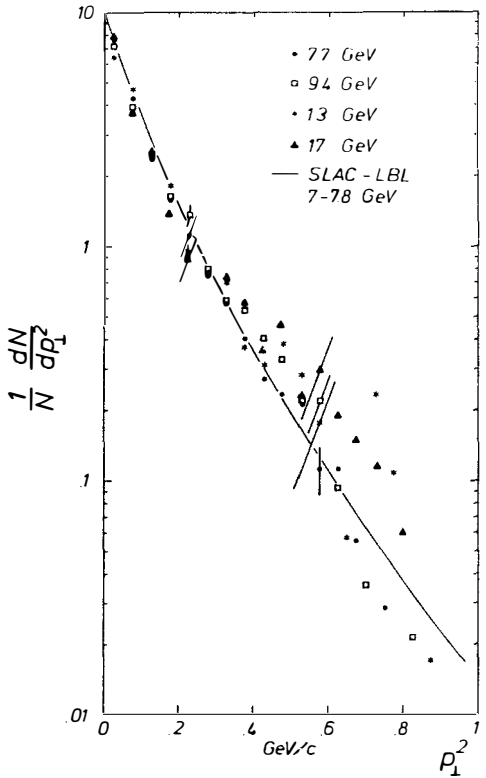

Fig. 8a: Distribution of the transverse momentum squared. The solid line is taken from ref. 1 and represents the $p_\perp^2$ distribution from the SLAC-LBL experiment at energies between 7 and 7.8 GeV. The data points are preliminary results from PLUTO.

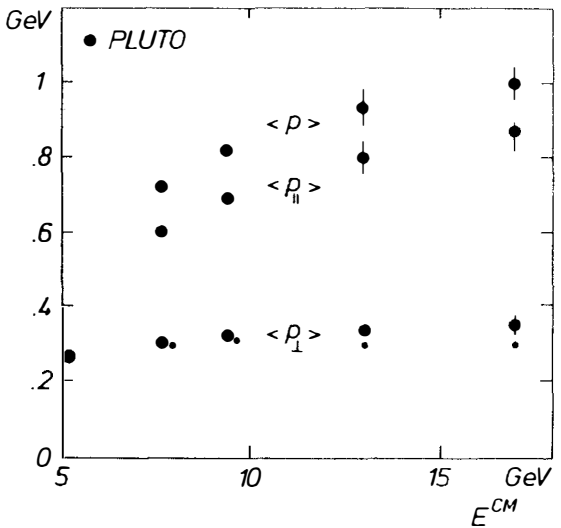

Fig. 8b: Average momentum of charged particles and of the components longitudinal and transverse to the jet axis. The small points are from the Feynman-Field $q\bar{q}$ Monte Carlo.

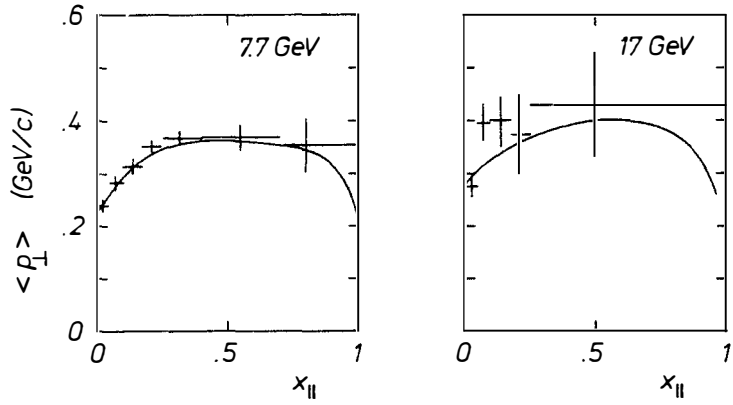

Fig. 9: Average transverse momentum versus $x_{\parallel}$ for PLUTO data at 7.7 and 17 GeV (preliminary). The curve is the Feynman-Field $q\bar{q}$ Monte-Carlo prediction.

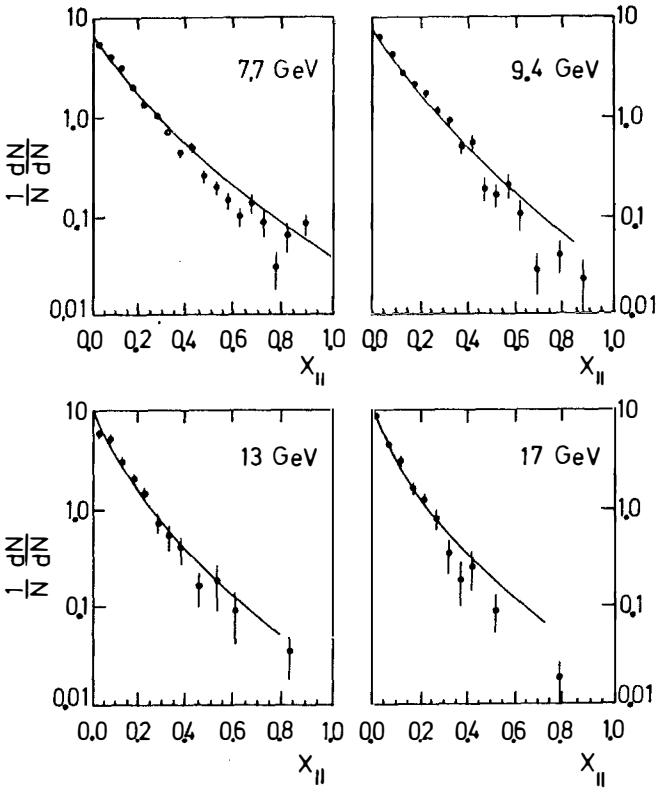

Fig. 10: Preliminary $x_{\parallel}$ distributions from PLUTO. The solid lines correspond to the Feynman-Field $q\bar{q}$ Monte Carlo.

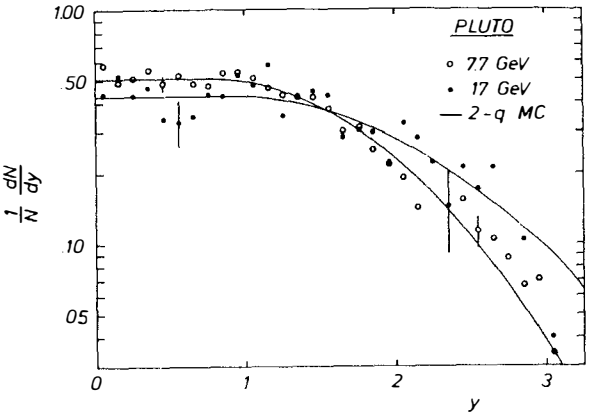

Fig. 11a: Rapidity distribution of PLUTO data at 7.7 and 17 GeV and Feynman-Field $q\bar{q}$ Monte-Carlo curves.

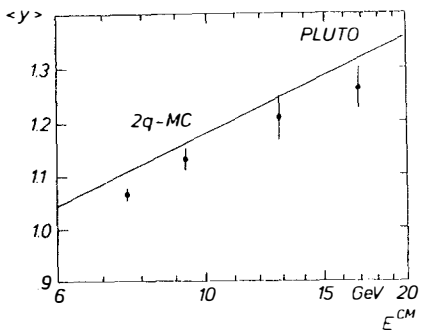

Fig. 11b: Energy dependence of the average rapidity.

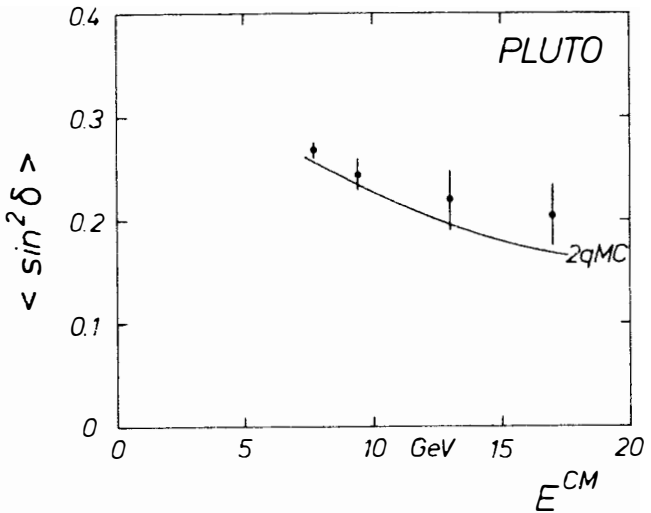

Fig. 12a: Average opening angle $\langle \sin^2\delta \rangle$ of energy flow in a jet.

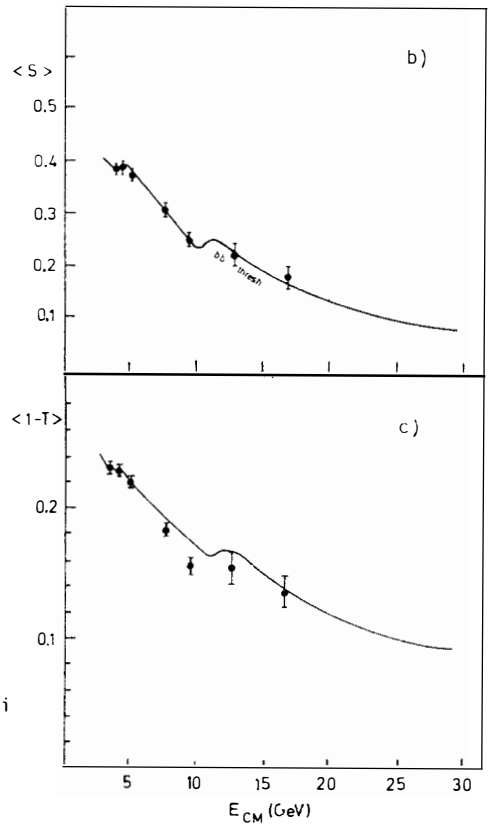

Fig. 12b and c: Average of sphericity and of (1-thrust). Solid curves are from a non perturbative $q\bar{q}$ model with u, d, s, c and b quarks (A. Ali et al.[9])

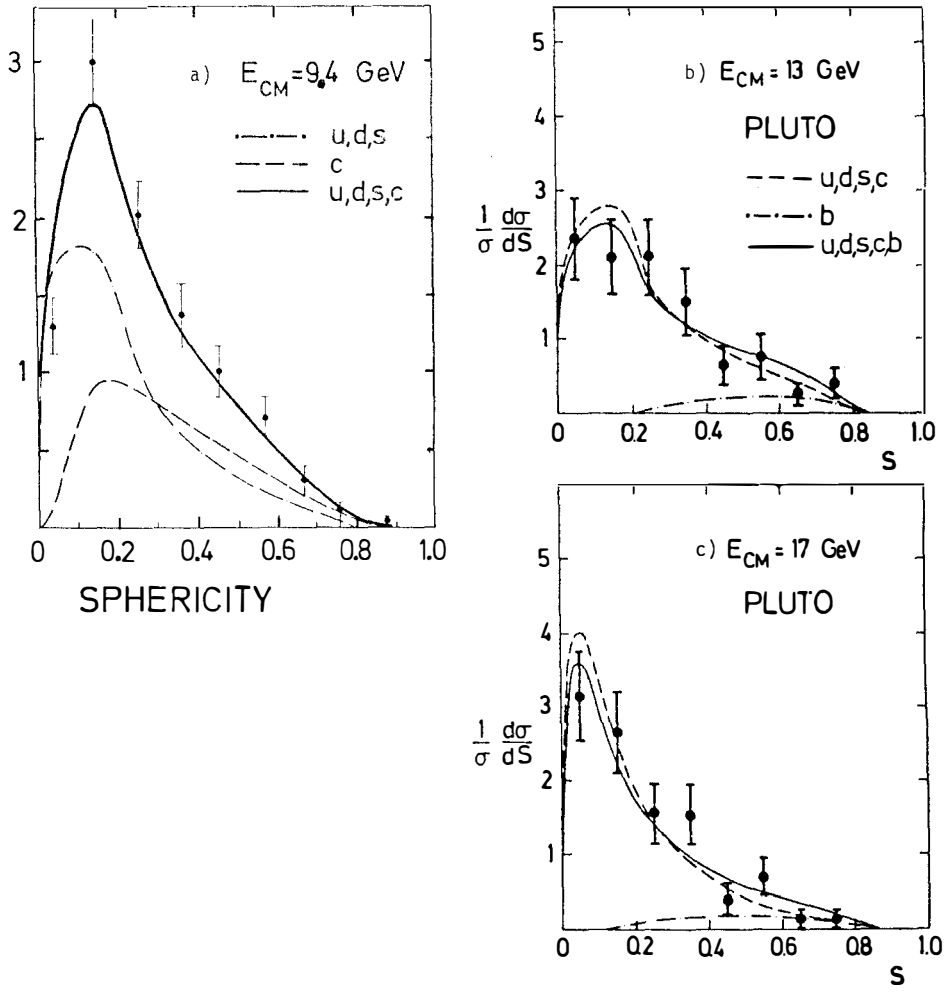

Fig. 13: Differential sphericity distributions at $\overline{Q} = 9.4$ (a), 13 (b), and 17 GeV (c). Curves are from ref. 9. In Fig. b and c the curves for (u, d, s, c) and (u, d, s, c, b) are each normalized to the data.

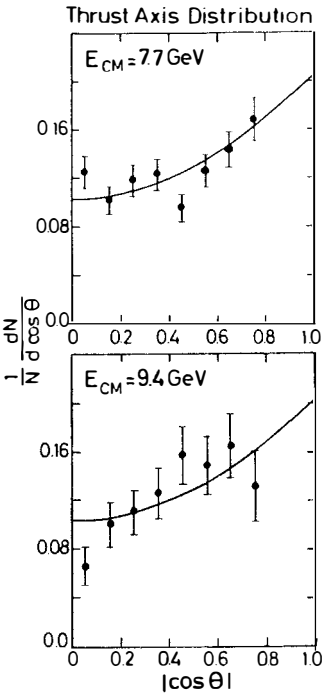

Fig. 14: Angular distribution of the jet axis. The curves are for $\alpha = 1$ in $dN/d\cos\theta \propto 1 + \alpha \cos^2\theta$.

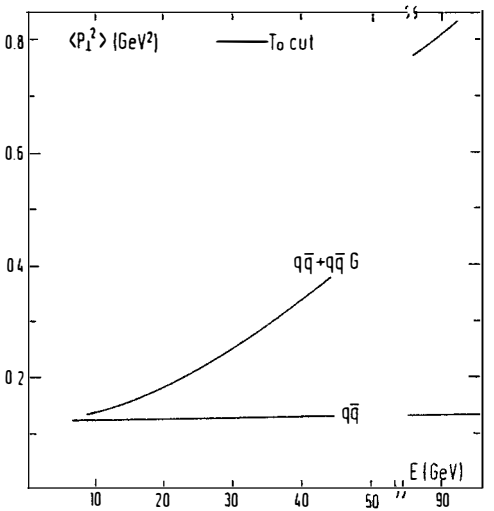

Fig. 15: QCD prediction (ref. 5) for the energy dependence of $\langle p_T^2 \rangle$.

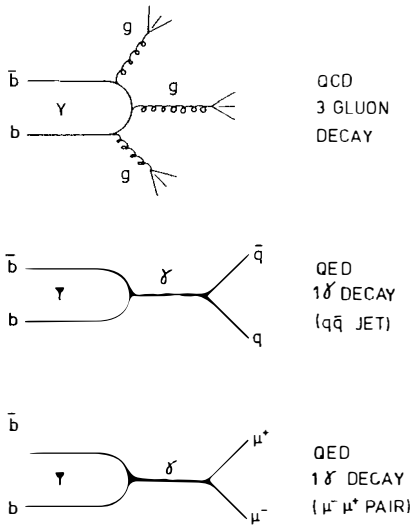

Fig. 16: Diagrams for the QCD and QED decay modes of the Υ(9.46).

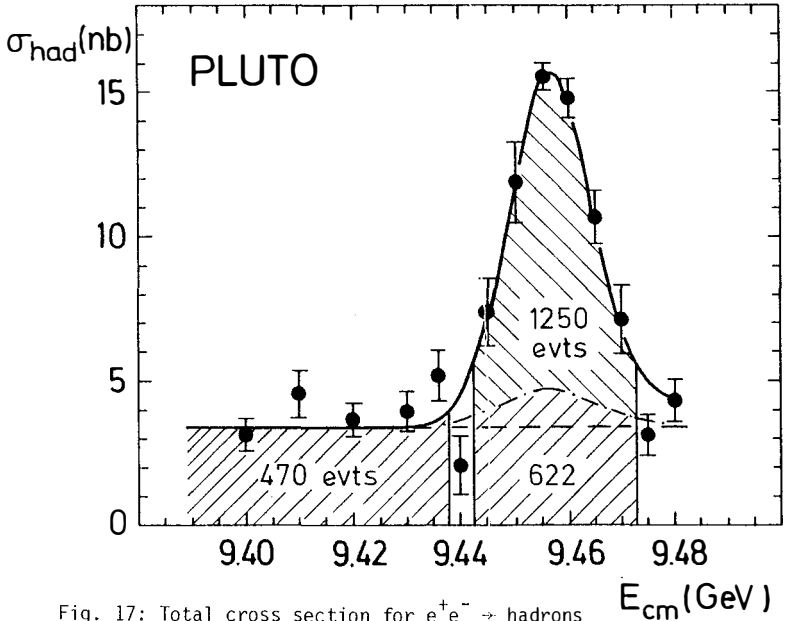

Fig. 17: Total cross section for $e^+e^- \to$ hadrons at energies around the Υ(9.46).

Fig. 18: Diagrams for $e^+e^- \to$ hadrons at the Υ(9.46) energy.

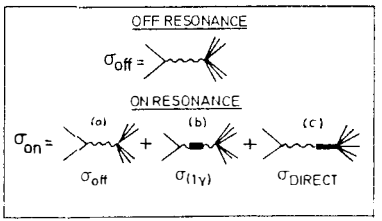

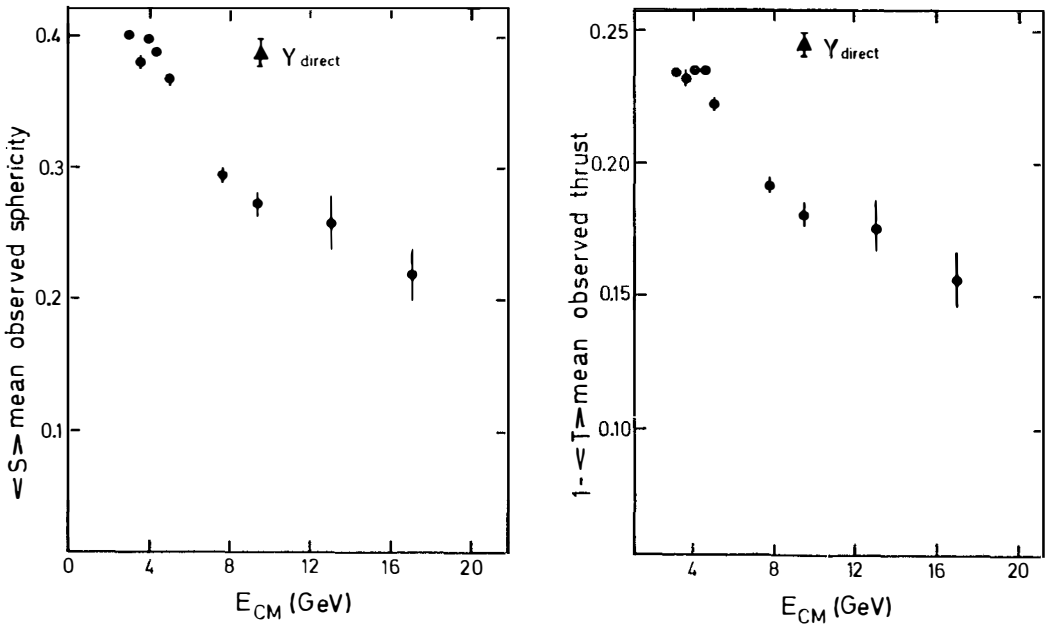

Fig. 19: Mean observed sphericity and thrust as function of energy.

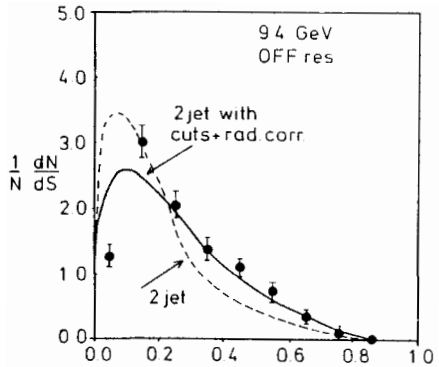

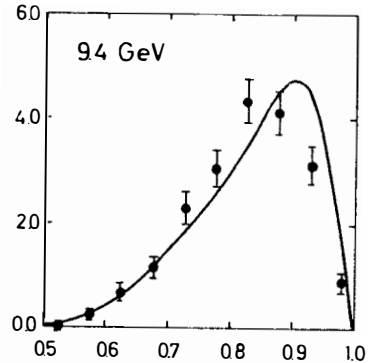

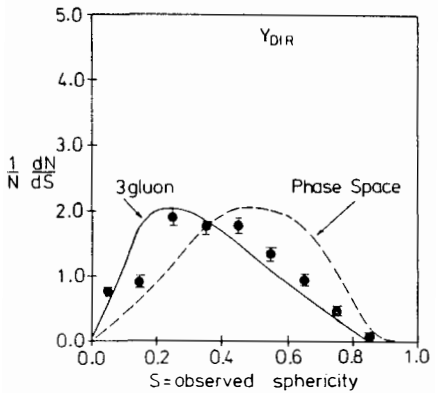

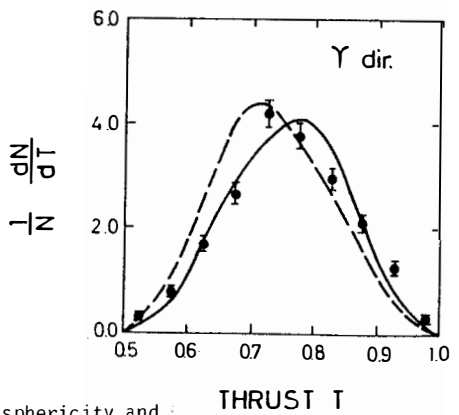

Fig. 20: Distribution of observed sphericity and observed thrust; off resonance, compared to the Feynman-Field $q\bar{q}$ model, and Υ_{direct} compared to phase-space and 3-gluon model.

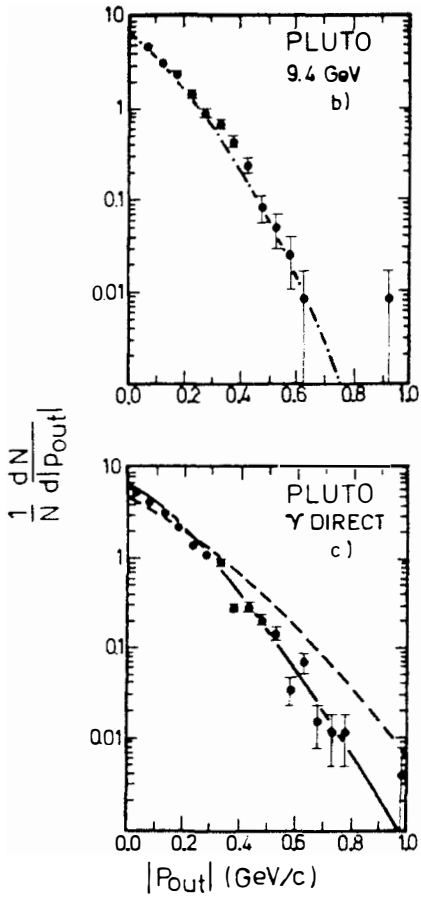

Fig. 21: Distribution of $|p_{out}|$ with respect to the Q_1 plane for off Υ and Υ_{direct}. Curves as in Fig. 20.

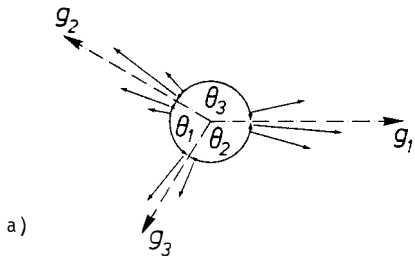

a)

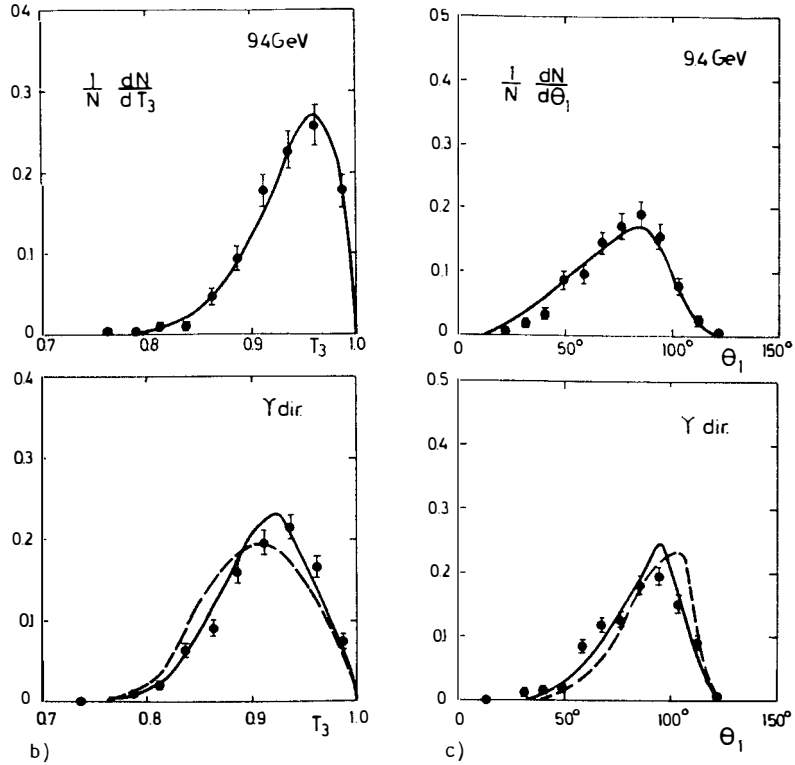

b) c)

Fig. 22: Triplicity plots; (a) definition of angles θ_i between the 3 triplicity axis g_ℓ, with the ordering $\theta_1 \leq \theta_2 \leq \theta_3$; (b) observed distribution of triplicity; (c) observed distribution of the (smallest) angle θ_1.

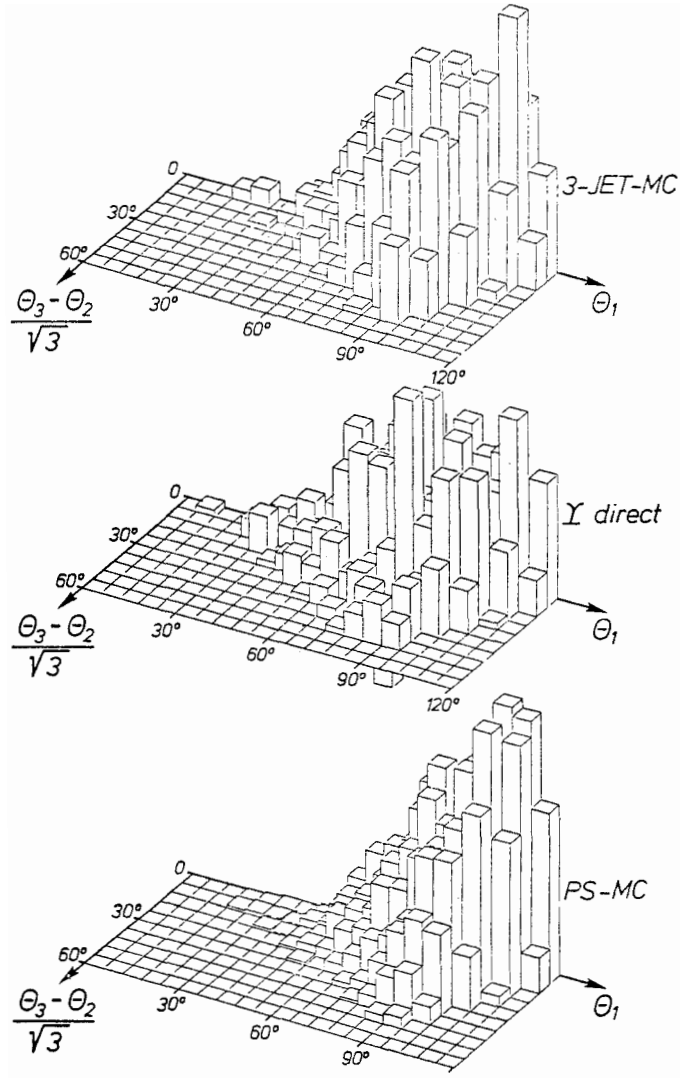

Fig. 23: Dalitz plot of the triplicity angles for Υ_{direct}, 3 g MC and phase space.